

# Dual-Wing Systems with Decalage Angle Optimization

Kamran Rokhsaz\* and Bruce P. Selberg†  
*University of Missouri—Rolla, Rolla, Missouri*

**Dual-wing general aviation designs are studied and compared with single-wing designs. It is demonstrated that with proper selection of gap, stagger, decalage, and mission requirements, total drag can be significantly reduced. Proper spanwise distribution of decalage is shown to enhance efficiency while raising the critical Mach number. Also, flight conditions have been chosen to result in operation at the proper Reynolds number, reducing the viscous drag even further.**

## Nomenclature

$A$	= wing reference area, $\text{ft}^2$
$\mathcal{R}$	= aspect ratio
$c$	= chord length, ft
$c_d$	= two-dimensional drag coefficient
$C_D$	= three-dimensional drag coefficient
$c_l$	= two-dimensional lift coefficient
$c_{l_0}$	= $c_l$ at zero angle of attack
$c_{l_\alpha}$	= $\partial c_l / \partial \alpha$
$C_L$	= three-dimensional lift coefficient
$c_m$	= two-dimensional pitching moment coefficient
$c_{m_\alpha}$	= $\partial c_m / \partial \alpha$
$C_p$	= pressure coefficient
$D$	= decalage angle, deg
$e$	= span efficiency factor
$G$	= gap
$H$	= altitude, ft
$M$	= Mach number
$R$	= Reynolds number/ft
$R_c$	= Reynolds number based on chord length
$S$	= stagger
$x$	= distance along chord from leading edge, ft
$W$	= total weight, lbf
$\alpha$	= angle of attack, deg
$\lambda$	= taper ratio
<i>Subscripts</i>	
$cr$	= critical
$opt$	= optimum
$r$	= wing root
$t$	= wing tip

## Introduction

RECENT studies have shown that closely coupled dual-wing systems possess aerodynamic advantages over the single-wing configurations. These could lead to dual-wing aircraft designs that are more fuel-efficient by virtue of their lower drag.

Several investigators have studied dual-wing systems,<sup>1-4</sup> with Nenadovitch<sup>5</sup> the first to discover improved two-dimensional characteristics. Olson and Selberg<sup>6</sup> and Rokhsaz<sup>7</sup>

Presented as Paper 84-2161 at the AIAA 2nd Applied Aerodynamics Conference, Seattle, WA, Aug. 21-23, 1984; submitted Oct. 4, 1985; revision received Feb. 10, 1986. Copyright © American Institute of Aeronautics and Astronautics, Inc., 1986. All rights reserved.

\*Teaching Fellow, Mechanical and Aerospace Engineering Department. Member AIAA.

†Professor of Aerospace Engineering, Mechanical and Aerospace Engineering Department. Associate Fellow AIAA.

showed that a dual-wing design could achieve substantially higher lift-to-drag ratios than its equivalent single-wing configuration. All these studies found the improved characteristics for  $S = 1.0$ ,  $G = 0.3$ , and  $D = -6$  deg. The definitions of stagger  $S$ , gap  $G$ , and decalage  $D$  are presented in Fig. 1. Wolkovitch<sup>8</sup> investigated tandem-wing systems. His experimental results illustrated the lower induced drag predicted by the Prandtl-Munk biplane theory.<sup>9,10</sup>

The studies carried out by the above investigators have all been limited either to two-dimensional flow or to wind tunnel tests at substantially lower than practical Mach and Reynolds numbers. Rhodes and Selberg<sup>11</sup> used a combination of the methods of Ref. 7 and vortex-lattice methods to optimize two general aviation designs. Although they substantiated the earlier findings at the same stagger, gap, and decalage, their results were limited to incompressible flow. However, they demonstrated that higher aspect ratios could be achieved for dual-wing designs without a weight penalty due to increased structural rigidity. This could further increase the aerodynamic efficiency of these designs.

The purpose of this paper is to reexamine the results of Ref. 11 in the presence of compressibility effects and to demonstrate the need for an optimized spanwise distribution of the decalage angle. At the same time, it is intended to show that Reynolds number can also be optimized to decrease the viscous drag further.

## Methods of Analysis

### Two-Dimensional

The two-dimensional analysis utilized the multielement vortex panel program of Ref. 7. The potential flow results of this program were used with momentum integral techniques to estimate the behavior of the boundary-layer flow over the airfoils. The laminar portion of the boundary layers were modeled with Thwaites' methods.<sup>12</sup> The transition points were located using Michel's criterion.<sup>13</sup> The method of Head and Cumpsty<sup>14</sup> was employed for turbulent boundary-layer calculations. Finally, the Squire-Young formula<sup>15</sup> was used to predict the viscous drag of each airfoil. The pressure coefficient was corrected for Mach number by the von Kármán-Tsien method<sup>16</sup> while Kaplan's method<sup>17</sup> was used for the lift coefficient.

This method allowed computation of complete two-dimensional aerodynamic coupling including the effect of the thickness of the airfoils, which can be significant at small gaps, as shown in Ref. 18.

### Three-Dimensional

Three-dimensional calculations were performed by using a vortex-lattice method that utilized the two-dimensional  $c_{l_0}$  and  $c_{l_\alpha}$  of the airfoils as predicted in the previous section. This method agreed well with Glauert's method<sup>19</sup> and the ex-

perimental results of Paulson<sup>20</sup> for single wings. Goethert's<sup>21</sup> similarity rules were used in this part to account for compressibility.

#### Optimization Method

The output from the above two- and three-dimensional programs was used in an optimization program that parametrically varied the wing area while calculating aircraft performance and searching for minimum cruise drag. The optimization program had weight equations calibrated with NASTRAN-SEMOBEAM results<sup>22</sup> for both single- and dual-wing designs.

### Discussion and Results

#### Airfoil Results

The airfoil chosen for this study was the NASA MS (1)-0313, which is of the newer medium-speed sections. Figure 2 shows a comparison of the experimental drag coefficient with that predicted by the present method at the design Reynolds number of 6 million. Similarly good results were obtained at other Reynolds numbers. The same section was used in a dual-airfoil configuration at  $R_c = 3 \times 10^6$  for comparison with the single-airfoil results at  $R_c = 6 \times 10^6$ . Three decalage angles were used at the optimum stagger of 1.0 and gap of 0.26. The results are shown in Fig. 3. The decalage angles of -4 and -6 deg offered 20-25% lower drag than the single airfoil, near the bottom of their drag buckets. The reason for this behavior is shown in Figs. 4 and 5. Figure 4 shows the pressure distribution over the airfoils at near-optimum lift coefficient. In the dual-airfoil configuration, both sections had a lower leading-edge suction than the single airfoil at the same lift coefficient. This resulted in a more favorable pressure gra-

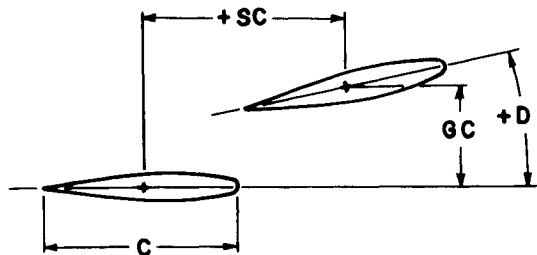


Fig. 1 Definitions of gaps and positive stagger and decalage.

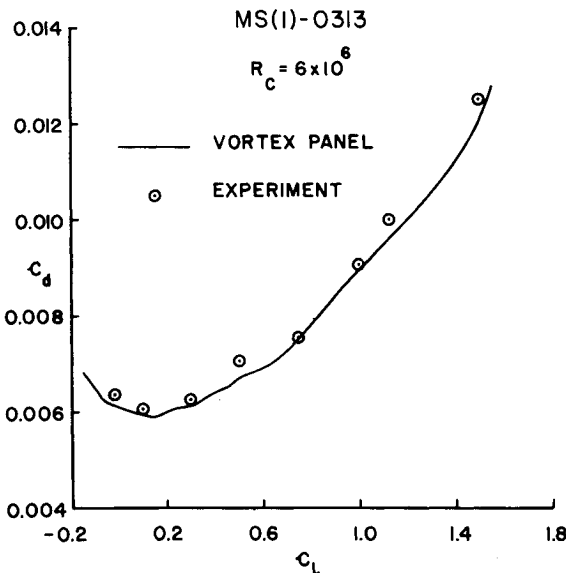


Fig. 2 Comparison of two-dimensional numerical with experimental results.

dient over the chord, leading to a delay in the boundary-layer transition. This delayed transition is demonstrated in Fig. 5 in comparison with the single airfoil at twice the chord Reynolds number. The results shown in Fig. 3 also demonstrate that the point of minimum drag shifted toward higher lift coefficients with increasing the magnitude of the decalage angle.

Figure 6 shows the estimates of the critical Mach number for the two-dimensional configurations considered here. The effect of decalage in all cases was to lower the absolute critical Mach number while shifting the peak toward higher lift coefficients.

#### Wing Results

Earlier studies<sup>23</sup> demonstrated an optimum taper ratio of 0.6 for the dual wings and 0.8 for the single wings. In this study, the effects of twist, decalage distribution, and Mach number on the induced drag were also studied.

Considering the airfoil drag and critical Mach number results presented in Figs. 3 and 6, respectively, it was concluded that the highest decalage angles had to be used near the wing root, where the lift coefficients were the highest. As the lift coefficient decreased near the wing tip, the decalage had to be decreased too in order to take advantage of the lower

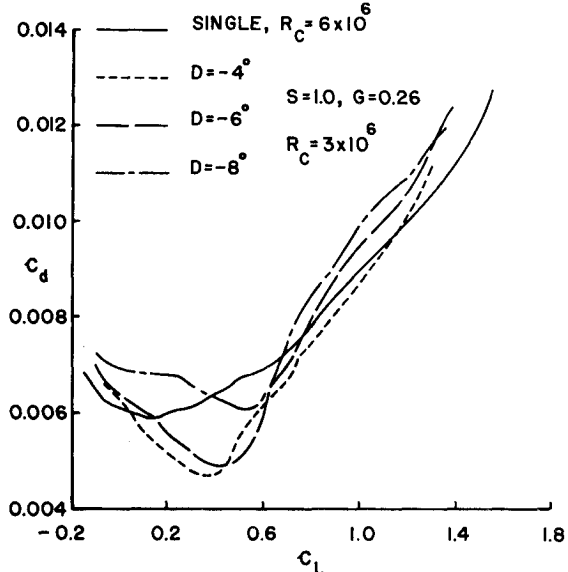


Fig. 3 MS(1)-0313 dual airfoil drag with decalage variation.

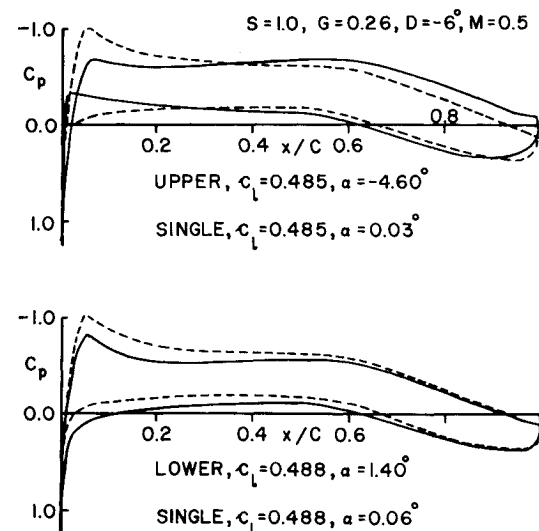


Fig. 4 MS(1)-0313 single- and dual-airfoil pressure distribution.

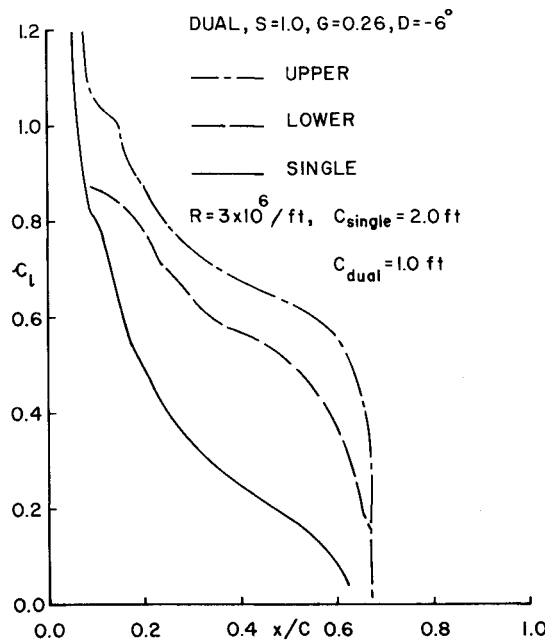


Fig. 5 Upper surface transition location for MS(1)-0313 airfoils.

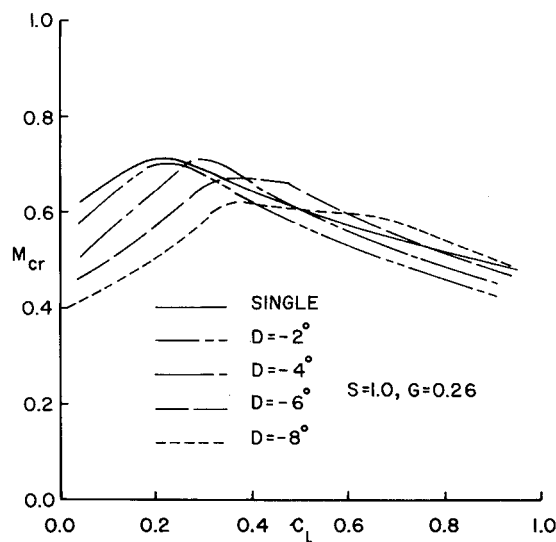


Fig. 6 Critical Mach number variation for single and dual MS (1)-0313 airfoils.

viscous drags. Furthermore, this would insure operations as far as possible from the estimated critical Mach number.

Span efficiency factor is shown in Fig. 7 for the single-wing case at different twist angles in comparison with a dual-wing design. It is quite clear that the dual-wing configuration has a much higher efficiency at all lift coefficients. Figure 8 shows the effect of twist on a dual-wing combination. The spanwise decalage distribution in this case has been tailored for minimum viscous drag. Only linear variation of decalage and twist were used. Figure 9 summarizes the same results for all the configurations considered here. In all cases, even when the dual and the single wings had the same aspect ratios, the dual-wing designs demonstrated higher span efficiency factors.

#### Airplane Results

Two classes of aircraft were analyzed; a six-passenger turboprop and a twelve-passenger twin turbofan. Since both aircraft demonstrated the same behavior, only the results for the six-place aircraft will be shown here.

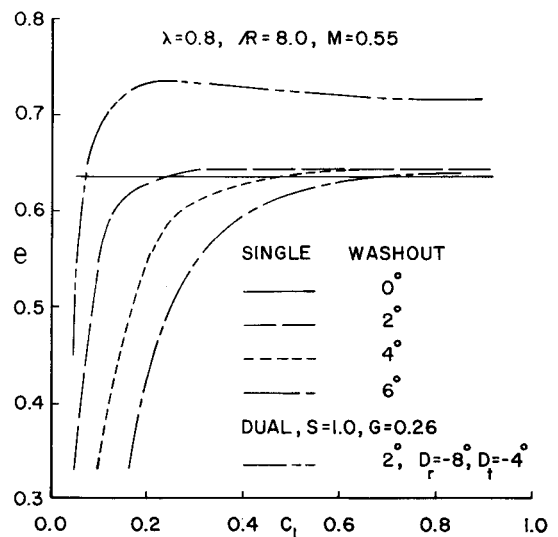


Fig. 7 Single-wingspan efficiency factor comparison with washout and optimized dual wing.

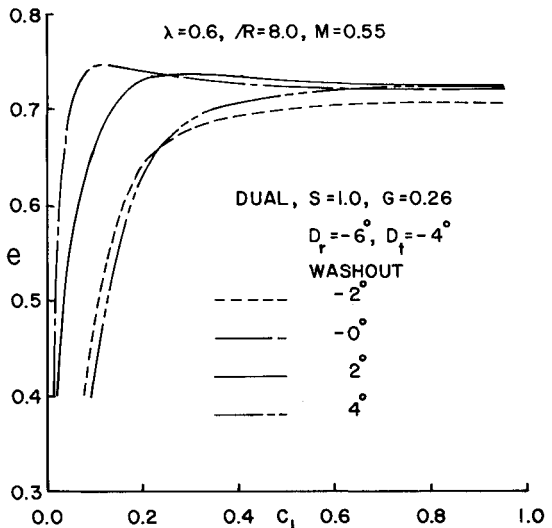


Fig. 8 Effect of washout on dual-wing span efficiency factor.

The details of the weight and fuselage are given in Ref. 24. The design specifications were chosen to permit operation close to the design Reynolds number of the MS(1)-0313 airfoil. They corresponded to flight Mach number of 0.55 at an altitude of 30,000 ft. Common fuselage, vertical and horizontal tails, and component weights were used for the dual- and single-wing designs. Also, the aerodynamic load of the horizontal tail was fixed. All aircraft were trimmed for positive lift on the tail for minimum induced drag as discussed by Kendall.<sup>24</sup> Since dual-wing airfoils have larger negative  $c_m$ <sup>5</sup> and  $c_{m_\alpha}$ <sup>18</sup> for positive stabilities, fixing the tail load penalized the dual-wing configurations. However, the drag penalty was estimated to be only of the order of 1% in terms of the total aircraft trim lift-to-drag ratio and was therefore ignored.

Aspect ratios of 8 and 12 were used for comparison. Since structurally a dual wing with aspect ratio of 16 compares with a single wing with aspect ratio of 12, these cases were also included in the analysis. For the dual-wing designs, decalage distribution of -6 deg at the wing root to -4 deg at the wing tip were deemed optimum. Although this decalage distribution did not offer the best efficiency, it allowed operation well below the estimated critical Mach numbers. In all cases, 2-deg washout produced the highest efficiency in the neighborhood

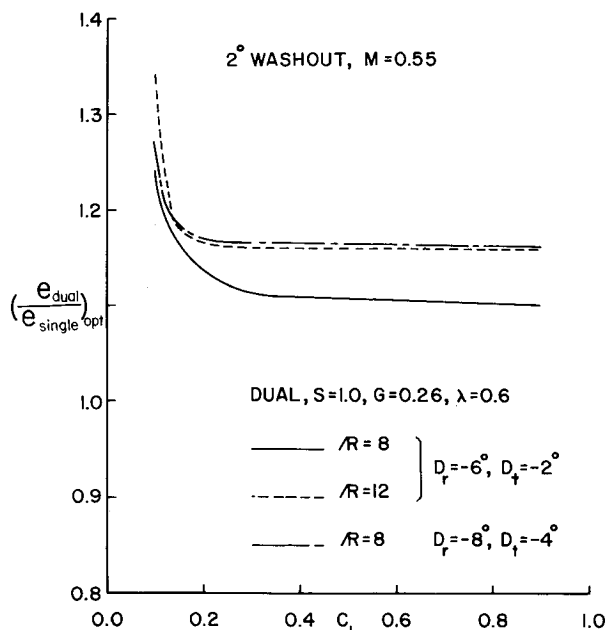


Fig. 9 Comparison of optimum dual- and single-wingspan efficiency factors.

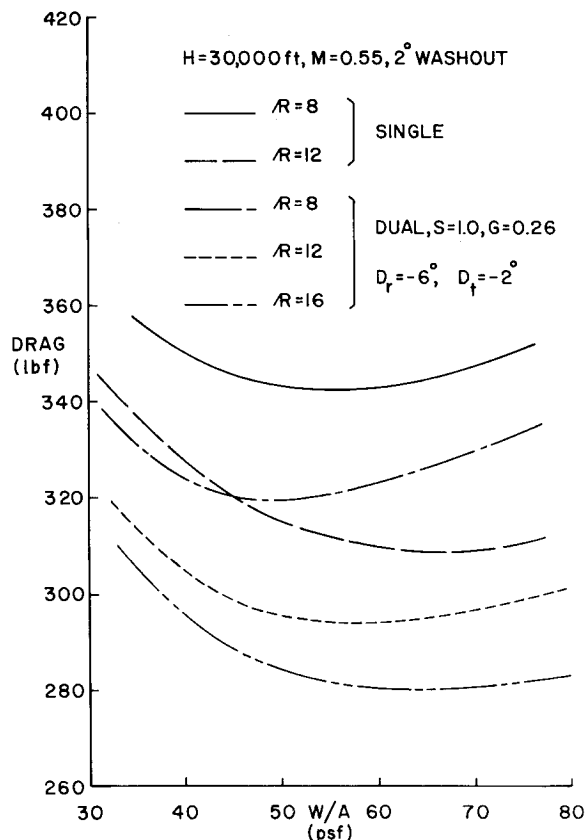


Fig. 10 Six-place aircraft cruise drag.

of the operational lift coefficient. Figure 10 shows the cruise drag of the six-place design as a function of the wing loading. In general, the optimum wing loading increased with aspect ratio. However, the optimum dual-wing designs allowed operation at a lower wing loading when compared with the equivalent single-wing designs. This behavior pointed out one of the advantages of the dual-wing configuration at higher aspect ratios where the optimum wing loading of the single-wing cases became rather excessive. As shown in this figure, it was also noted that for wing loading of less than 45 psf, the

Table 1 Aerodynamic characteristics of optimized configurations

	Single wing		Dual wing		
	AR = 8	AR = 12	AR = 8	AR = 12	AR = 16
Weight, lbf	3926	3958	3954	3979	4012
W/A, psf	54.6	60.0 <sup>a</sup>	49.2	58.6	60.0 <sup>a</sup>
$C_L$	0.41	0.45	0.37	0.44	0.45
Drag, lbf	344	310	321	296	281
$R_c \times 10^{-6}$	4.7	3.7	2.5	1.9	1.6
Altitude = 30,000 ft, $M = 0.55$ , six-place design					

<sup>a</sup>Arbitrarily limited wing loading.

dual-wing design with aspect ratio of 8 is superior to the single-wing designs of aspect ratio 12. Also, as the aspect ratio increased, the total drag became less sensitive to wing loading. This allowed the placement of an arbitrary upper limit of 60 psf on the wing loading of all designs without greatly increasing the total drag

Quantitatively comparing these configurations at aspect ratio of 8 with the optimum wing loading, a total drag reduction of 6.5% was achieved by the dual-wing system. Also, comparison of the dual-wing design of aspect ratio 12 with the single-wing case of aspect ratio 8 revealed 14% lower drag. This comparison is justified due to the fact that the dual wings of aspect ratio 12 had the same structural characteristics as the single wings with aspect ratio of 8

Table 1 presents the characteristics of the final six-place design. These results indicated drag savings substantially higher than those presented in Ref. 11. These differences are attributed to the proper choice of Reynolds number, spanwise variation of the decalage angle, and twist. As mentioned earlier, similar results were observed for the twelve-place design.

These studies were limited to constant engine and fuel weights. Lower power requirements of the dual-wing systems can allow these weights to be decreased.

### Conclusions

Aerodynamic efficiencies of two classes of dual-wing aircraft were studied and compared with the performance of optimum equivalent single-wing designs. In all cases, using numerical techniques, the dual-wing configurations were optimized for the best combinations of decalage and Reynolds number with considerations for compressibility effects. In every respect, the dual-wing systems proved to be more efficient.

### References

- 1 Norton, F.H., "Effect of Staggering a Biplane," NACA TN-710, 1918.
- 2 Knight, M. and Noyes, R.W., "Wind Tunnel Test on a Series of Biplane Wing Models, Part I. Effects of Changes in Stagger and Gap," NACA TN-310, 1929.
- 3 Knight, M. and Noyes, R.W., "Wind Tunnel Test on a Series of Biplane Wing Models, Part II. Effects of Changes in Decalage, Dihedral, Sweepback, and Overhand," NACA TN-325, 1929.
- 4 Knight, M. and Noyes, R.W., "Wind Tunnel Test on a Series of Biplane Wing Models, Part III. Effects of Changes in Various Combinations of Stagger, Gap, and Decalage," NACA TN-330, 1929.
- 5 Nenadovitch, M., "Recherches sur les Cellules Biplane Rigides d'Envergure Infine," *Publication Scientifique et Techniques du Ministere de L'Air*, Institut Aero'-technique de Saint-Cyre, Paris, 1936.
- 6 Olson, E. C. and Selberg, B. P., "Experimental Determination of Improved Aerodynamic Characteristics Utilizing Biplane Wing Configurations," *Journal of Aircraft*, Vol. 13, April 1976, pp. 256-261.
- 7 Rokhsaz, K., "Analytical Investigation of the Aerodynamics Characteristics of Dual Wing Systems," University of Missouri-Rolla, 1980.
- 8 Volkovitch, J., "Subsonic V/STOL Configurations with Tandem Wings," *Journal of Aircraft*, Vol. 16, Sept. 1979, pp. 605-611.
- 9 Munk, M. M., "General Biplane Theory," NACA Report 151, 1922.

<sup>10</sup>Prandtl, L., "Induced Drag of Multiplanes," NACA TN-182, 1924.

<sup>11</sup>Rhodes, M. D. and Selberg, B.P., "Benefits of Dual Wings Over Single Wings for High Performance Business Airplanes," *Journal of Aircraft*, Vol. 21, Feb. 1984, pp. 116-127.

<sup>12</sup>Thwaites, B., "Approximate Calculation of the Laminar Boundary Layer," *Aeronautical Quarterly I*, 1949.

<sup>13</sup>Michel, R., "Etude de la Transition sur les Profiles d'Ails; Establisment d'un Critere de Determination de Point de Transition et Calcul de la Trainee de Profile Incompressible," ONERA Rept. 1/1578A, 1951.

<sup>14</sup>Dvorak, F. A. and Woodward, F. A., "A Viscous/Potential Flow Interaction Analysis Method for Multi-Element Infinite Swept Wings, Vol. I," NASA CR-2476, 1974.

<sup>15</sup>Cebeci, T. and Smith, A. M. O., "Calculation of Profile Drag of Airfoils at Low Mach numbers," *Journal of Aircraft*, Vol. 5, Nov.-Dec. 1968, pp. 535-542.

<sup>16</sup>Anderson, J., *Fundamentals of Aerodynamics*, McGraw-Hill Book Co., New York, 1984, pp. 421-423.

<sup>17</sup>Abbott, I. H. and Von Doenhoff, A. E., *Theory of Wing Sections*, Dover Publications, New York, 1959, pp. 256-261.

<sup>18</sup>Rokhsaz, K. and Selberg, B. P., "Disadvantages of Thin Airfoil Formulations for Closely Coupled Airfoils," *Journal of Aircraft*, Vol. 20, June 1983, pp. 574-576.

<sup>19</sup>Kuethe, A. M. and Schetzer, J. D., *Foundations of Aerodynamics*, John Wiley & Sons, New York, 1959, pp. 107-111.

<sup>20</sup>Paulson, J. W., "Application of Vortex Lattice Theory to Preliminary Aerodynamic Design," NASA TN-D-8236, 1976.

<sup>21</sup>Shapiro, A. H., *The Dynamics and Thermodynamics of Compressible Fluid Flow*, Vol. I, Ronald Press, New York, 1953, pp. 316-325.

<sup>22</sup>Somnay, R. J., "Design of Dual Wing Structures," M.S. Thesis, University of Missouri-Rolla, 1983.

<sup>23</sup>Rhodes, M. D., "Advantages of Dual Wing Aircraft Designs," M.S. Thesis University of Missouri-Rolla, 1982.

<sup>24</sup>Kendall, E. R., "The Minimum Induced Drag, Longitudinal Trim and Static Longitudinal Stability of Two-Surface and Three-Surface Airplanes," AIAA Paper 84-2164, Aug. 1984.

*From the AIAA Progress in Astronautics and Aeronautics Series..*

**AEROACOUSTICS:**

**JET NOISE; COMBUSTION AND CORE ENGINE NOISE—v. 43**

**FAN NOISE AND CONTROL; DUCT ACOUSTICS; ROTOR NOISE—v. 44**

**STOL NOISE; AIRFRAME AND AIRFOIL NOISE—v. 45**

**ACOUSTIC WAVE PROPAGATION;**

**AIRCRAFT NOISE PREDICTION;**

**AEROACOUSTIC INSTRUMENTATION—v. 46**

*Edited by Ira R. Schwartz, NASA Ames Research Center, Henry T. Nagamatsu, General Electric Research and Development Center, and Warren C. Strahle, Georgia Institute of Technology*

The demands placed upon today's air transportation systems, in the United States and around the world, have dictated the construction and use of larger and faster aircraft. At the same time, the population density around airports has been steadily increasing, causing a rising protest against the noise levels generated by the high-frequency traffic at the major centers. The modern field of aeroacoustics research is the direct result of public concern about airport noise.

Today there is need for organized information at the research and development level to make it possible for today's scientists and engineers to cope with today's environmental demands. It is to fulfill both these functions that the present set of books on aeroacoustics has been published.

The technical papers in this four-book set are an outgrowth of the Second International Symposium on Aeroacoustics held in 1975 and later updated and revised and organized into the four volumes listed above. Each volume was planned as a unit, so that potential users would be able to find within a single volume the papers pertaining to their special interest.

v. 43—648 pp., 6 x 9, illus.	\$19.00 Mem.	\$40.00 List
v. 44—670 pp., 6 x 9, illus.	\$19.00 Mem.	\$40.00 List
v. 45—480 pp., 6 x 9, illus.	\$18.00 Mem.	\$33.00 List
v. 46—342 pp., 6 x 9, illus.	\$16.00 Mem.	\$28.00 List

*For Aeroacoustics volumes purchased as a four-volume set: \$65.00 Mem. \$125.00 List*

**TO ORDER WRITE:** Publications Order Dept., AIAA, 1633 Broadway, New York, N.Y. 10019